

RESEARCH ON PLANT SAMPLING SYSTEM IN COMPLEX GEOGRAPHICAL ENVIRONMENT USING UAV

基于无人机的复杂地理环境植物采样系统研究

Juyong ZHANG^{1✉}, Minquan ZHOU¹, Kai HE^{1,2}, Minkang GUO¹, Guohao LI³, Rong LI^{1✉}

¹) School of Mechanical Engineering, Hangzhou Dianzi University, Hangzhou 310017, China;

²) National Astronomical Observatories, CAS, Beijing 100101, China;

³) Zhuji CANU Automation Equipment Co., Ltd, Shaoxing 311800, China

Tel: +86 13735525761, +8615658883283; E-mail: zhang_juyong01@163.com, lirongjx@hdu.edu.cn

Corresponding authors: Juyong Zhang, Rong Li

DOI: <https://doi.org/10.35633/inmateh-67-16>

Keywords: Plant Sampling; Unmanned Aerial Vehicle; Plant sampling manipulator; Design & experiment

ABSTRACT

Aiming at the difficult problem of contact sampling of plant in complex geographical environment, a remote-controlled sampling method using an Unmanned Aerial Vehicles (UAV) is proposed. After configuration, mechanism parameter analysis & optimization, and dynamic analysis, a special lightweight sampling manipulator that integrates plant stem-and-leaf sample capture, cutting and storage is designed. The designed sampling manipulator is composed of a ball screw nut transmission pair and a symmetrical double-offset slider rocker. The minimum transmission angle of the rocker is 63.435° , the maximum opening displacement of the manipulator claw is 131 mm, and the cutting pressure is 226 N. Tests and experiments show that the sample manipulator has a mass of 2.35 kg, a cutting pressure of 214 N, and a maximum open displacement of the manipulator claws of 126 mm. It can be controlled locally or remotely using a UAV to grab, cut and storage plant samples with a diameter greater than 5 mm. The reliability of the sampling manipulator design and the feasibility of the sampling method are verified.

摘要

针对复杂地理环境下植物样本接触式取样作业困难的问题,提出了一种基于无人机平台、可远程操控的取样方法。通过构型、机构参数分析与优化及动力学分析,设计了一款集植物茎叶样本抓取、切割与收贮一体化专用轻巧的取样机械手。设计的取样机械手由滚珠丝杠螺母传动副和对称双偏置滑块摇杆串联构成,摇杆最小传动角 63.435° ,机械手爪最大张开位移 131mm,切割压力 226N。经测试和试验表明,取样机械手样机质量 2.35Kg,切割压力达 214N,机械手爪最大张开位移为 126mm,能在本地或基于无人机平台远程操控,进行样本茎秆直径的抓取、切割与收贮一体化采集作业,验证了取样机械手设计的可靠性与取样方法的可行性。

INTRODUCTION

Plant sampling is the basic work of production and scientific and technological activities such as agricultural and forestry resource investigation, pest control, growth monitoring and botany research. Plant sampling is divided into two types: non-contact plant data information collection and contact plant sampling. At present, with the development of telemetry technologies such as vision and image processing, satellite and UAV remote sensing, spatial positioning and communication, non-contact plant information collection has made great progress in level of intelligence, real-time monitoring capabilities, and systematic management (Sladojevic et al., 2016; Peña-Barragán et al., 2014; Trang et al., 2020; Xu et al., 2021; Wang et al., 2019; NIU et al., 2018; Sun et al., 2018). In terms of contact plant sampling, tools and equipment such as branch shears and excavation have been studied in driving methods and optimizing mechanical transmission routes, which have effectively improved the comfort and efficiency of manual on-site sampling. In agricultural and forestry manipulators, a lot of progress has also been made in the research of agriculture and forestry fruit picking by manipulators (Xia et al., 2016; Meng et al., 2016; Peng et al., 2018). However, compared with non-contact plant information data collection, the development of contact plant sampling technology and equipment is relatively slow. Plant sampling in complex geographic environments such as mountainous areas, rivers, lakes and swamps lacks effective automation and intelligent sampling equipment, sampling operations are difficult, or even difficult to successfully collect.

This paper mainly aims at the difficulties in contact sampling of stems, branches and leaves, or aquatic phytoplankton plants in complex geographic environments, and lack of automated sampling equipment, etc., and proposes a remotely controlled contact sampling method for plant samples using a UAV. Carrying out the configuration and parameter optimization design and dynamic analysis of the special sampling manipulator for this sampling method, and passing the prototype performance test and sampling test, lay the technical foundation for the development of the plant contact automatic sampling system.

MATERIALS AND METHODS

Plant sampling method using UAV

In complex geographical environments such as cliffs in mountainous areas, rivers, lakes and swamps in plains, in order to realize automated plant sample contact sampling, it is necessary to focus on the design of special manipulators for plant contact sampling, safe commuting to and from the sampling operation site, and remote control.

At present, UAV has developed to the level of consumption, with its superior hovering manoeuvrability, intelligent remote control, has been more and more widely used in the field of non-contact plant information collection of agricultural and forestry crops growth, yield prediction, pest control and quality detection (Cao *et al.*, 2020; Murefu *et al.*, 2019; Raeva *et al.*, 2019; Zhao *et al.*, 2019; Shi *et al.*, 2017; Yang *et al.*, 2015). The professional-grade UAV has a load capacity of more than 5 kg and a battery life of more than 40 minutes (DJI Innovations, 2019), which can provide a good platform foundation for commuting to and from the complex geographic environment. However, the airborne capacity of UAV is still very limited. Therefore, in this paper, sampling devices less than 3 kg and plant sampling less than 2 kg are set as specification.

For the contact sampling of stems, branches and leaves, and aquatic phytoplankton, according to the manual operation mode, the functional actions can be decomposed into three basic functional actions: the grabbing of the stems and leaves (or aquatic phytoplankton), the stems and leaves and the parent body (or the surrounding phytoplankton) cutting and separating, sample storage. Correspondingly, the special sampling manipulator needs to realize the functional actions of three sampling operations. The shear characteristics of plant stalks are affected by many factors such as variety, diameter, maturity, and water content (Ma *et al.*, 2019), and the cutting and separating power of aquatic phytoplankton is also affected by factors such as variety and flourishing degree. In this paper, 200 N is set as the design target of the shearing and separating pressure of the sampling manipulator to realize the sampling operation requirements of 5 mm plant stem cutting or phytoplankton separation.

Choose a UAV with a suitable remote controller model to control the UAV commute to and from the sampling site. At the same time, with the cooperation of the UAV video system, the sampling manipulator can realize remote control of plant sampling by a remote controller.

Therefore, the technical solution of contact sampling of plant samples that can be remotely controlled using a UAV proposed in this paper is shown in Figure 1. Under the control of remote controller, the UAV was suspended with a sampling manipulator to enter the sampling site in a complex geographical environment. The sampling manipulator grabs, cuts, separates and stores the plant samples, and then the UAV brings the samples back, so as to realize the plant contact sampling in a complex geographical environment.

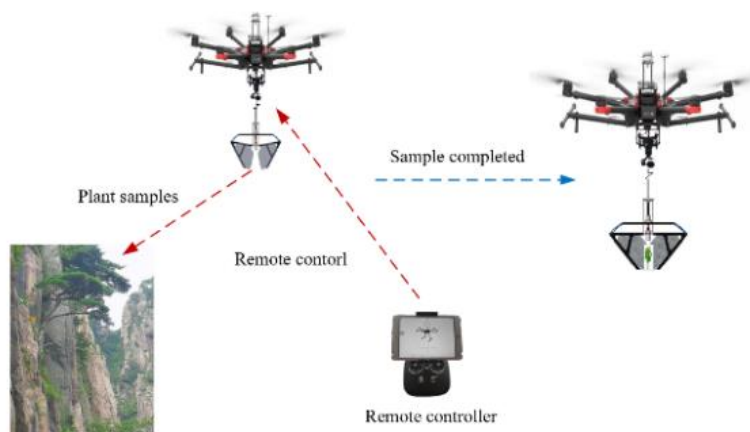


Fig. 1 - Schematic diagram of plant sampling method in complex geographic environment using UAV

Design of sampling manipulator

The UAV can be selected and configured through the market, and the remote control technology is mature and reliable. However, the special sampling manipulator for grabbing plant sample, cutting and separating, and storing and other functions is limited due to UAV airborne capacity. Smart and lightweight design are the technical keys to the realization of the sampling method using the UAV proposed in this paper.

Configuration design

The sampling manipulator needs to have integrated design of grabbing, cutting and separating, and storing to realize all the functional actions of plant sampling. The configuration diagram and mechanism parameters of the sampling manipulator in this paper are shown in Figure 2. The sampling manipulator is a type of series combined mechanism which consists of a ball screw nut transmission pair and a symmetrical double offset slider rocker. When the ball screw nut rises, the symmetrical double offset slider is driven to rise, and the two symmetrical rockers swing upward at the same time, so that the angle of the symmetrical rocker-type robotic arm is opened, and at the end of the robotic arm the manipulator claws that are formed by the cutting blades are displaced and opened, which facilitates the plant samples to enter the manipulator; on the contrary, when the ball screw nut drops, the symmetrical mechanical arm angles are closed, and the manipulator claws grab and clamp the plant samples. When the angle of the robotic arm is closed to a certain angle, the blades of the robotic claw begin to shear and separate the stalks of the sample; the sheared and separated samples are stored in the robotic arm and returned with the UAV to complete the sampling.

Mechanism parameter design and optimization analysis

The design parameters of the sampling manipulator mechanism are shown in Figure 2. They are the length of the rocker x_1 , the length of the connecting rod x_2 , and the symmetrical offset of the slider x_3 . When the symmetrical manipulator is closed, the vertical height between the slider and the base is x_4 , the displacement of the ball screw (*i.e.*, the total stroke of the slider) is x_5 , the vertical height between the manipulator claw and the base is x_6 , when the symmetrical manipulator arm is closed. If the rocker rotation angle, the transmission angle and the angle between the slider and the connecting rod are expressed as α , γ and β respectively, when the two extreme positions of the robot arm for maximum opening and closing (*that is*, the ball screw nut is at the uppermost end and the lowermost end), there are formula 1 and formula 2:

$$x_2 \cos \beta + \sqrt{x_1^2 - (x_2 \sin \beta + x_3)^2} - x_4 - x_5 = 0 \quad (1)$$

$$(x_1 - x_3)^2 + x_4^2 - x_2^2 = 0 \quad (2)$$

In the sampling manipulator, the maximum opening angle of the manipulator (or the maximum horizontal displacement y_{max} of the manipulator claw) will determine the maximum grabbing space range of the manipulator, which depends on the rocker rotation angle α_{max} of the double offset slider rocker mechanism, that is the design parameters of the mechanism. At the same time, the grabbing and cutting pressure of the manipulator claw changes with the displacement of the ball screw. When the ball screw nut moves down, the manipulator closes and grabs the sample until it is cut and separated. When the manipulator is closed, the rocker transmission angle is the minimum value y_{min} . At the moment, if the transmission angle γ_{min} of the rocker is greater, the transmission force performance for sample grabbing and cutting is better, which means that the slider rocker mechanism transmits the driving force to the manipulator claw (Wang *et al.*, 2018).

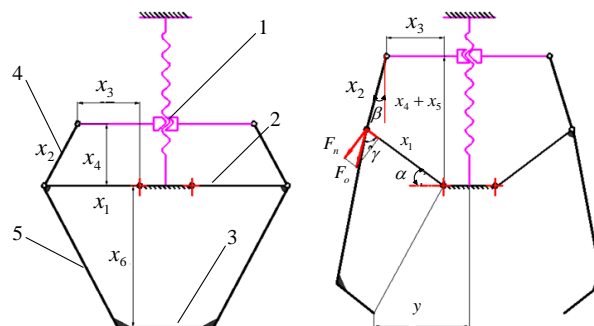


Fig. 2 - The motion diagram and design parameters of the sampling manipulator configuration

1. Ball screw nut pair 2. Rocker 3. Cutting blade 4. Robotic arm 5. Connecting rod

According to the schematic diagram of the design parameters in Figure 2, the optimization objective function formulas of the minimum rocker transmission angle γ_{min} and the maximum rocker rotation angle α_{max} (or the maximum horizontal displacement of the manipulator claw opening) can be derived as formula 3 and formula 4:

$$\alpha(x)_{max} = \arcsin \frac{x_4 + x_5 - x_2 \cos \beta}{x_1} \quad (3)$$

$$\begin{cases} y(x)_{max} = x_6 \sin \alpha_{max} = x_6 \times \frac{x_4 + x_5 - x_2 \cos \beta}{x_1} \\ \gamma(x)_{min} = \arccos \frac{x_3^2 + (x_4 + x_5)^2 - x_1^2 - x_2^2}{2x_1x_2} \end{cases} \quad (4)$$

The sampling manipulator is a combination mechanism of a ball screw nut drive pair and a symmetrical double offset slider rocker in series. The value range of the design parameter variables should meet the motion performance of the offset slider rocker mechanism, that is they should meet formula 5 and formula 6.

$$g_1(x) = x_1 + x_3 - x_2 > 0 \quad (5)$$

$$g_2(x) = x_1 + x_2 - x_3 > 0 \quad (6)$$

In order to narrow the search range of the optimized objective function, according to the structural layout and preliminary parameter design, the minimum rocker transmission angle $\gamma_{min} \geq 40^\circ$ and the maximum open displacement $y_{max} \geq 50 \text{ mm}$ of the manipulator claw are added as the constraint conditions of the inequality when solving, as shown in formula 7:

$$g_3(x) = \begin{cases} \arccos \frac{x_3^2 + (x_4 + x_5)^2 - x_1^2 - x_2^2}{2x_1x_2} - 40^\circ \geq 0 \\ x_6 \times \frac{x_4 + x_5 - x_2 \cos \beta}{x_1} - 50 \geq 0 \end{cases} \quad (7)$$

Mechanism parameter design and optimization results

There are 5 independent variables in the parameter design of the sampling manipulator mechanism, which are the length x_1 of the rocker, the symmetrical offset x_3 of the slider, the vertical height x_4 between the slider and the base (*when the robotic arm is closed*), and the displacement x_5 of the ball screw (i.e., the total stroke of the slider), the vertical height x_6 between the manipulator claw and the base (*when the manipulator is closed*). The length x_2 of the connecting rod of the slider rocker mechanism is the amount of strain x_1 , x_3 and x_4 .

According to the requirements of sampling manipulator sampling storage space, structural layout and reducing parameter optimization solution calculation amount, the mechanism parameters x_4 , x_5 and x_6 are designed as constant values, which are 60 mm, 90 mm and 150 mm respectively. The parameter x_1 and x_3 are used as the design variable, and the minimum rocker transmission angle γ_{min} and the maximum horizontal displacement y_{max} of the manipulator claw opening (*i.e., the maximum rocker rotation angle α_{max}*) are used as the optimization targets, and the optimization analysis and solution of the two design variables x_1 and x_3 are carried out.

In this paper, ADAMS/View is used as the simulation optimization platform, according to the optimization analysis formula of the mechanism parameters above, the kinematics simulation model of the sampling manipulator mechanism is established, and the optimized objective measurement function curve and optimization constraints shown in Figure 3 are created.

According to the sample storage space requirements and constraints of the sampling manipulator, the initial values of the design variables of the rocker length x_1 and the symmetrical offset x_3 of the slider are 150 mm and 50 mm respectively, and the value ranges are 150-185 mm and 50-150 mm respectively. After design sensitivity analysis for variables optimization, the design variable x_1 is used as the main optimization parameter and the optimization analysis step length is taken as 5 mm to optimize the value of variables x_1 and x_3 and carry out the kinematics optimization analysis of the mechanism (Zhang et al., 2015).

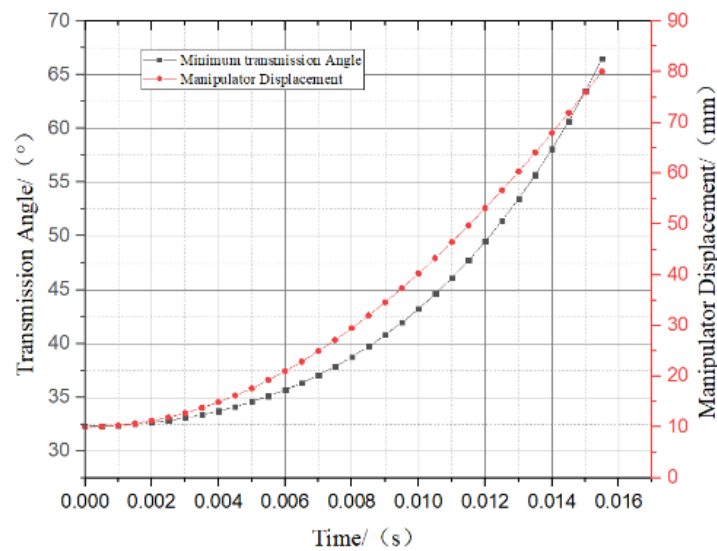


Fig. 3 - Optimize the target measurement function curve

Figure 4 shows the results of the optimization target parameters corresponding to the values of the design variables. It can be seen from it that the maximum opening displacement y_{max} of the manipulator claw is 111.86 mm corresponding to the initial values of the design variables x_1 and x_3 , but the minimum rocker transmission angle γ_{min} of 38.66° doesn't meet the design target requirement. According to the optimized analysis results in Figure 4, under the premise of meeting the design targets, the sample storage space should be increased as much as possible, that is, x_1 and x_3 must be as large as possible. They are finally taken as 185 mm and 150 mm respectively, and the corresponding minimum rocker transmission angle γ_{min} and the maximum opening displacement y_{max} of manipulator claw is 63.435° and 131 mm respectively. Compared with the initial 30.66°, γ_{min} increased by 106.8%, which greatly improves the force transmission efficiency of the mechanism. The maximum open displacement y_{max} of the manipulator claw is 18.14 mm larger than the initial 111.86 mm, which is better than the design target of 100 mm.

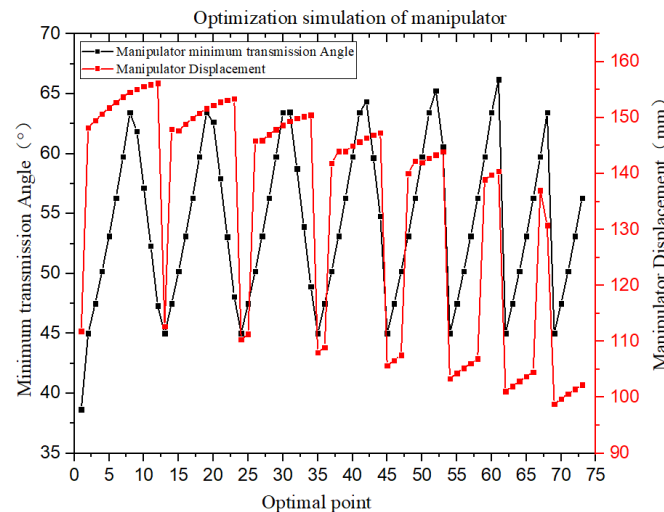


Fig. 4 - Selection of Design Variables of Sampling Manipulator and Optimal Analysis Results

Dynamic analysis of sampling manipulator

After designing and optimizing the parameters of the sampling manipulator mechanism, in the structure, the robotic arm is equipped with connecting rods to improve the rigidity, the structure is hollowed out, and carbon fibre CFRP with higher specific strength and thermoplastic resin PA66 materials are selected to realize the lightweight structure. After the structural design is completed, the dynamic simulation model shown in Figure 5 is established on the ADAMS platform to analyse and check whether the cutting pressure and opening horizontal displacement of the manipulator claw meet the design targets, and to provide a basis for the subsequent selection of the drive motor.

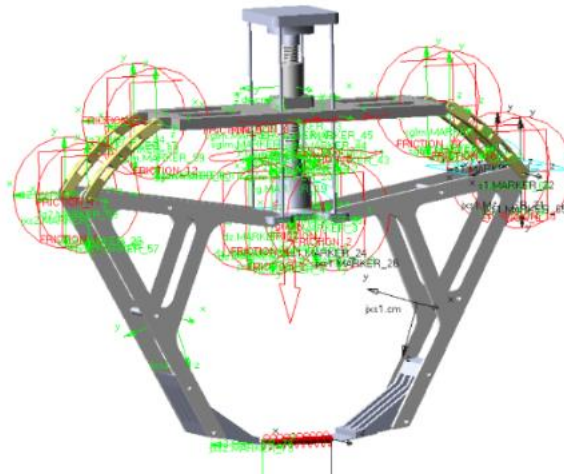


Fig. 5 - Dynamic simulation model of sampling manipulator

In the simulation process, according to the torque parameters of the alternative motor drive of the sampling manipulator, torques are created in the analysis model to simulate the motor drive of the sampling manipulator. Set up a virtual spring to simulate the cutting resistance of the manipulator claw. In the simulation analysis, an acceleration sensor is established. When the acceleration of the screw nut is 0 (*i.e.*, the manipulator claw is in the state of maximum cutting pressure), the simulation analysis calculation stops. Figure 6 shows the curves of the force measurement results of the manipulator claw spring simulator and the results of the manipulator claw displacement analysis under different driving torques. It can be seen from Figure 6 that the maximum opening displacement of the manipulator claw is 131 mm, which meets the 100 mm requirement of the design index of the grabbing space. When the driving torque of the drive motor is 250 N·mm, the maximum cutting pressure of the manipulator claw is 226 N, which can meet the design target of 200 N, that is, the torque of the selected drive motor should not be less than 250 N mm.

In the simulation, when the cutting pressure of the manipulator claw is equal to the spring force of the simulated spring, the spring force is the maximum cutting pressure of the manipulator claw. At this moment, the acceleration is zero, and the robotic arm bears the maximum shear resistance; in the simulation, there is no obvious sudden change in the curve of the robotic arm displacement and cutting pressure, indicating that the movement process of the sampling manipulator structure is relatively stable (*Li et al., 2015*).

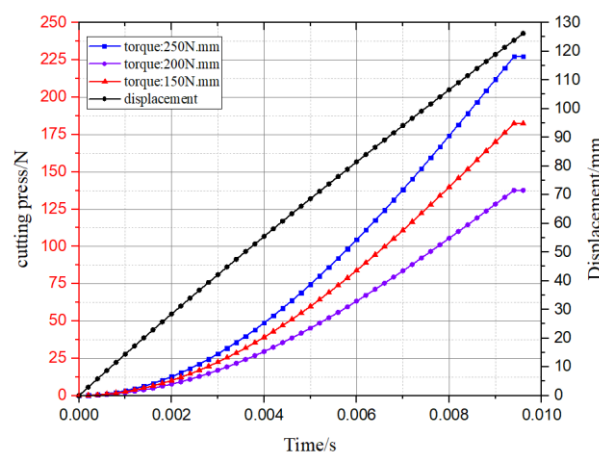


Fig. 6 - Sampling manipulator drive torque and cutting separation force measurement and analysis results

RESULTS

Sampling manipulator prototype

The actual sample of the sampling manipulator is shown in Figure 7. It is mainly composed of a drive motor, a ball screw nut transmission pair, a symmetrical double offset slider rocker structure in series, a robotic arm fixedly connected with the rocker, and manipulator claw is composed of a cutting blade at the end of the robotic arm, and the grid storage cover. The overall structural mass of the sampling manipulator is 2.35 kg, which has reached the lightweight design target; the maximum open displacement of the manipulator claw is 126 mm, which is consistent with the simulation analysis results.

Performance test and experiment of sampling

Manipulator cutting pressure test and local sample collection experiment

Set up the manipulator claw cutting pressure test platform as shown in Figure 7.

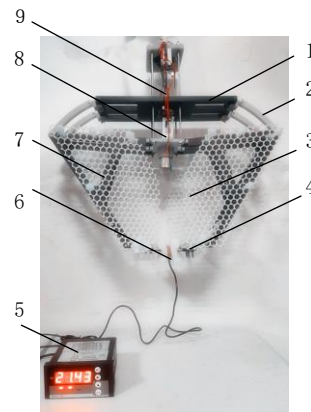


Fig. 7 - Sampling robot prototype and cutting force test

1. Slider; 2. Connecting rod; 3. Net bag; 4. Cutting blade; 5. Digital display instrument; 6. Pressure sensor; 7. Robotic arm; 8. Limit switch 9. Ball screw nut

During the test, first start the drive motor to open the robotic arm, place the pressure sensor between the manipulator claws, and then start the drive motor to reverse to simulate the cutting operation of the sampling manipulator grabbing plant samples. When the drive motor starts to block, the maximum cutting pressure of the manipulator claw is reached, the value of the cutting pressure is recorded by the digital display instrument matched with the pressure sensor. The range of the cutting pressure test value of the sampling manipulator is 214 ± 1 N, which has reached the design target of 200 N. Compared with the result 226 N of dynamic simulation analysis, it is 25% smaller, which is mainly caused by factors such as the assembly accuracy of the sampling manipulator and the friction of the mechanism motion pair.

In order to further test the cutting, grasping and storage performance of the prototype for plant samples, field random sampling experiments of Camellia, Nandin, Melilotus, Photinia and Arisaema are carried out, as shown in figure. 8.



Fig. 8. Sampling plant samples

In the experiment, the manipulator uses the same type of cutting blade, each sample experiment 20 times. The experimental results are shown in Table 1. The experimental results show that the sampling manipulator realizes the cutting design target of sample stem diameter $\geq 5\text{ mm}$. As the obstruction of surrounding stems and leaves increases, it will be more difficult to grab samples, which is related to the lightweight design of the sampling manipulator, which doesn't have enough weight. After cutting, the samples can be stored naturally in the manipulator without sample omission.

Table 1

Local sampling results of the manipulator

	Stem diameter			Ease of operation	
	[mm]			[%]	
	Median	Max	Min	Grab	Store
Camellia	4.4	5.8	3.9	75	100
Nandin	4.8	5.5	4.1	80	100
Melilotus	5.2	6.2	4.4	80	95
Photinia	4.8	5.5	3.8	70	100
Arisaema	4.6	5.9	3.9	75	100

Remote control sampling test using UAV



Fig. 9 - Sampling system and sampling test using UAV

Figure 9 shows the sampling system and sampling test after the sampling manipulator is suspended under a UAV through a sling. With the support of the video surveillance system carried by the UAV, the operator remotely controls the sampling manipulator to grab, cut and separate samples of the stems, branches and leaves of Du Ying's canopy. The separated stems, branches and leaves samples are stored in the sampling robotic arm, and return with the UAV to complete the sampling operation. In the experiment, the linear distance between the operator and the sampling location, the height, and the diameter of the sample stem are shown in Table 2.

Sampling test results using UAV

Table 2

	Sampling location and operation location		Stem diameter	
	[m]		[mm]	
sampling location	distance	height	Max	Min
1	47	13	6.1	3.8
2	64	20.5	5.7	3.7
3	158	11.5	5.4	4.6
4	192	16	6.3	5.2
5	207	29	5.8	4.2
6	334	28	5.2	4.9

The experimental results show that the stems, branches and leaves of samples can enter the robotic arm smoothly, then the robotic arm closes to grab and cut, and the samples return with the UAV in the robotic arm to complete the sampling. The maximum diameter of the sample stem is 6.3 mm, which has reached the design target ≥ 5 mm of this paper. The distance between the sampling location and the operator ranges from more than 40 meters to more than 300 meters, realizing the target of remotely controlling sampling. Its distance mainly depends on remote control performance of UAV and controller.

CONCLUSIONS

This paper proposes a plant contact sampling method using a UAV, which can realize remote control of plant sampling, thereby providing a solution for solving the difficulty of plant contact sampling in a complex geographic environment.

According to the proposed plant contact sampling method, this paper designed a sampling manipulator composed of a ball screw nut drive pair and a symmetrical double-offset slider rocker in series to realize sampling operation design of integrating grabbing, cutting and storing plant samples such as stems, branches, and leaves. Through the optimization analysis of kinematic mechanism parameters with the minimum transmission angle of the double-offset slider rocker and the maximum opening displacement of the manipulator claw as the optimization objectives, the optimization results of the transmission angle of 63.435° and the opening displacement of 131 mm are obtained. Through dynamic modelling analysis, it is proved that the sampling cutting pressure is 226 N, when the driving torque of the manipulator is 250 N mm.

Through the local test of the prototype, the overall structure mass of the sampling manipulator is 2.35 kg, the maximum open displacement of the manipulator claw is 126 mm, and the cutting pressure is 214 N. The sample stem diameter ≥ 5 mm can be grabbed, cut, and collected, which verified the light weight and reliability of the sampling manipulator design.

Through remote control sampling test using UAV, the plant sampling ability of the remote control of the prototype system is confirmed, thus verifying the feasibility of the sampling method in this paper.

Research will be carried out on the adjustment of the grasping direction of the manipulator according to the posture of the sampled target, so as to be more conducive to the grasping situation in the real scene where the sampled target is not growing vertically.

The manipulator is suspended under the UAV by a sling. The downward swirling airflow of the UAV and the wind in the real environment will affect the manipulator and the sample target. The gripping control of the manipulator under such interference conditions will be studied.

ACKNOWLEDGEMENT

This research was funded by Basic Public Welfare Research Project of Zhejiang Province of China (Grant No. LGN20E050004), the Zhejiang Province Science and Technology Development Funds (Grant No.2020C01061).

Thanks to Ruibin Yan and Aiguo Yin for assistance in controlling and using the UAV. We also thank Xue Zhao for assistance in writing and editing.

REFERENCES

- [1] Cao L., Liu K., Shen X. et al. (2020), Estimation of Forest Structural Parameters Using UAV-LiDAR Data and a Process-Based Model in Ginkgo Planted Forests[J]. *IEEE Journal of Selected Topics in Applied Earth Observations and Remote Sensing*, 12(11):4175-4190.
- [2] DJI Innovations. (2019), Jingwei M600PRO integrates great foresight [EB/OL]. <https://www.dji.com/cn/matrice600-pro>.
- [3] Li H., Chao W.B., Li S.F., et al. (2015), Kinematics Analysis and Experiment of Automatic Seedling Extraction Mechanism for Pepper Plug Seedlings [J]. *Transactions of the Chinese Society of Agricultural Engineering*, 31(23):20-27. (In Chinese with English abstract).
- [4] Ma X.L., Chen X.Y., Yan Y.S. et al. (2012), Mechanical damage test and biomechanical properties of bayberry [J]. *Transactions of the Chinese Society of Agricultural Engineering*, 28(16):282-287. (In Chinese with English abstract).
- [5] Meng C. (2020), Design and experiment of a new type of multi-degree-of-freedom high-branch pruning manipulator [J]. *Chinese Journal of Agricultural Machinery Chemistry*, 41(3):67-73. (In Chinese with English abstract).

- [6] Murefu Mike, Chen Shengbo. (2019), Assessing applicability of Near-Infrared/Green/Blue UAV modified camera in crop monitoring: a case study of eastern Zimbabwe[J]. *Global Geology*, 22(02):34-40.
- [7] Niu Yaxiao, Zhang Liyuan, Han Wenting. (2018), Extraction Methods of Cotton Coverage Based on Lab Colour Space. *Transactions of the Chinese Society for Agricultural Machinery*, 49 (10):240-249 (In Chinese with English abstract).
- [8] Peña-Barragán José, Gutiérrez Pedro Antonio, Martínez Cesar Hervás et al. (2014), Object-Based Image Classification of Summer Crops with Machine Learning Methods[J]. *Remote Sensing*, 6(6).
- [9] Peng Y., Liu Y.G., Yang Y. et al. (2018), Research Progress on the Application of Soft Manipulator Claw in Fruit and Vegetable Picking [J]. *Transactions of the Chinese Society of Agricultural Engineering*, 34(9):11-20.
- [10] Raeva P.L., Jaroslav Šedina, Dlesk A. (2019), Monitoring of crop fields using multispectral and thermal imagery from UAV [J]. *Nephron Clinical Practice*, 52(sup1):192-201.
- [11] Shi J., Feng Z., Liu J. (2017), Design and experiment of high precision forest resource investigation system based on UAV remote sensing images [J]. *Nongye Gongcheng Xuebao/Transactions of the Chinese Society of Agricultural Engineering*, 33(11):82-90. (In Chinese with English abstract).
- [12] Sladojevic S., Arsenovic M., Anderla A. et al. (2016), Deep Neural Networks Based Recognition of Plant Diseases by Leaf Image Classification [J]. *Computational Intelligence and Neuroscience*, 2016:1-11.
- [13] Sun Y., Zhou Y., Yuan M. et al. (2018), UAV real-time monitoring for forest pest based on deep learning [J]. *Nongye Gongcheng Xuebao/Transactions of the Chinese Society of Agricultural Engineering*, 34(21):74-81. (In Chinese with English abstract).
- [14] Trang K., Long T.T., Nguyen G.M.T. (2020), Plant Leaf Disease Identification by Deep Convolutional Autoencoder as a Feature Extraction Approach[C]. *The 17th IEEE International Conference on Electrical Engineering /Electronics, Computer, Telecommunications and Information Technology*. IEEE,
- [15] Wang X.W., Wu M.H., Zhou J. et al. (2018), Optimization and simulation of structure parameters of famous tea picking robot manipulator[J]. *Chinese Journal of Agricultural Machinery Chemistry*, 39(7):84-89. (In Chinese with English abstract).
- [16] Wang S.S., Wang S., Zhang H. et al. (2019), Weed recognition in soybean field based on lightweight sum product network and UAV remote sensing image [J]. *Transactions of the Chinese Society of Agricultural Engineering*, 35(06):89-97.
- [17] Xia C., Cao Q., Yang Y. (2016), Optimization design on end effector of grafted seedlings transplanting robot [J]. *Journal of Chinese Agricultural Mechanization*, 37(009):37-42. (In Chinese with English abstract).
- [18] Yang G.J., Li C.C., Yu H.Y. et al. (2015), Agricultural UAV multi-sensor remote sensing assisted wheat breeding information acquisition [J]. *Transactions of the Chinese Society of Agricultural Engineering*, 31(21):184-190. (In Chinese with English abstract).
- [19] Zehai Xu, Haiyan Song, Zhiming Wu, et al. (2021), Research on Crop Information Extraction of Agricultural UAV Images Based on Blind Image Deblurring Technology and SVM [J]. *INMATEH-Agricultural Engineering*, 64(2):33-42.
- [20] Zhang YL, Wang WX, Ma B, et al. (2015), Mechanism design and parameter optimization of cotton picking manipulator [J]. *Agricultural Mechanization Research*, (3):142-145. (In Chinese with English abstract).
- [21] Zhao J.L., Jin Y., Ye H.C. et al. (2020), Remote sensing monitoring of betel nut yellowing disease based on UAV multi-spectral image [J]. *Transactions of the Chinese Society of Agricultural Engineering*, 36(8):54-61. (In Chinese with English abstract).